Inorg. Chem. **2007**, *46*, 6083–6090

Formation and Characterization of Co(III)–Semiquinonate Phenoxyl Radical Species

Yuichi Shimazaki,*,† Ryota Kabe,§ Stefan Huth,‡,|| Fumito Tani,† Yoshinori Naruta,† and Osamu Yamauchi*,§

Institute for Materials Chemistry and Engineering, Kyushu University, Higashi-ku, Fukuoka 812-8581, Japan, Unit of Chemistry, Faculty of Engineering, Kansai University, Suita, Osaka 564-8680, Japan, and Department of Chemistry, Graduate School of Science, Nagoya University, Chikusa-ku, Nagoya 464-8602, Japan

Received March 29, 2007

Co(III) complexes of N_3O-donor tripodal ligands, 2,4-di(*tert*-butyl)-6-{[bis(2-pyridyl)methyl]aminomethyl}phenolate (tbuL), 2,4-di(*tert*-butyl)-6-{[bis(6-methyl-2-pyridyl)methyl]aminomethyl}phenolate (tbuL(Mepy)$_2$), were prepared, and precursor Co(II) complexes, [Co(tbuL)Cl] (**1**) and [Co(tbuL(Mepy)$_2$)Cl] (**2**), and ternary Co(III) complexes, [Co(tbuL)(acac)]ClO_4 (**3**), [Co(tbuL)(tbu-cat)] (**4**), and [Co(tbuL(Mepy)$_2$)(tbu-SQ)]ClO_4 (**5**), where acac, tbu-cat, and tbu-SQ refer to pentane-2,4-dionate, 3,5-di(*tert*-butyl)catecholate, and 3,5-di(*tert*-butyl)semiquinonate, respectively, were structurally characterized by the X-ray diffraction method. Complexes **3** and **5** have a mononuclear structure with a *fac*-N_3O_3 donor set, while **4** has a *mer*-N_3O_3 structure. The cyclic voltammogram (CV) of complex **3** exhibited one reversible redox wave centered at 0.93 V (vs Ag/AgCl) in CH_3CN. Complex **5** was converted to a phenoxyl radical species upon oxidation with Ce(IV), showing a characteristic π–π^* transition band at 412 nm. The ESR spectrum at low temperature and the resonance Raman spectrum of **3** established that the radical species has a Co(III)–phenoxyl radical bond. On the other hand, the CVs showed two oxidation processes at $E_{1/2} = 0.01$ and $E_{pa} = 0.92$ V for **4** and $E_{1/2a} = 0.05$ and $E_{1/2b} = 0.69$ V for **5**. The rest potential of **4** (–0.11 V) was lower than the $E_{1/2}$ value, whereas that of **5** (0.18 V) was higher, indicating that the first redox wave of **4** and **5** is assigned to the tbu-cat and the tbu-SQ redox process, respectively. One-electron oxidized **4** showed absorption, resonance Raman, and ESR spectra which are similar to those of **5**, suggesting formation of a stable Co(III)–semiquinonate species, which has the same oxidation level of **5**. The resonance Raman spectrum of two-electron oxidized **4** showed the ν_{8a} bands of the semiquinonate and phenoxyl radical, which were absent in the spectrum of one-electron oxidized **5**. Since both oxidized species were ESR inactive at 5 K, the former was concluded to be a biradical species containing semiquinonate and phenoxyl radicals coupled antiferromagnetically and the latter to a species with a coordinated quinone.

Introduction

A coordinating tyrosyl radical has been identified in the active site of galactose oxidase (GOase), which contains one copper ion and performs the oxidation of a primary alcohol to the aldehyde in the presence of dioxygen.[1−5] From the standpoint of coordination chemistry, one-electron oxidation of transition-metal complexes with a coordinated phenolate may be either a metal- or a ligand-centered reaction.[6] We have investigated the properties of some kinds of metal−phenoxyl radical species. The reaction of $Cu(ClO_4)_2 \cdot 6H_2O$ with N_2O_2-donor ligands containing two phenol moieties gave Cu(II)−phenoxyl radical species by disproportionation.[7,8] Oxidation of a low spin d^8 Ni(II)−salen complex

* To whom correspondence should be addressed. E-mail: yshima@ms.ifoc.kyushu.ac.jp (Y.S.). Fax: +81-6-6330-3770 (O.Y.). osamuy@ipcku.kansai-u.ac.jp (O.Y.).

† Kyushu University.

§ Kansai University.

‡ Nagoya University.

|| On leave of absence from the University of Bremen.

(1) (a) Whittaker, J. W. *Met. Ions Biol. Syst.* **1994**, *30*, 315. (b) Whittaker, J. W. In *Bioinorganic Chemistry of Copper*; Karlin, K. D., Tyeklár, Z., Eds.; Chapman & Hall: New York, 1993; p 447.

(2) (a) Itoh, N.; Phillips, S. E. V.; Stevens, C.; Ogel, Z. B.; McPherson, M. J.; Keen, J. N.; Yadav, K. D. S.; Knowles, P. F. *Nature* **1991**, *350*, 87. (b) Itoh, N.; Phillips, S. E. V.; Stevens, C.; Ogel, Z. B.; McPherson, M. J.; Keen, J. N.; Yadav, K. D. S.; Knowles, P. F. *Faraday Discuss.* **1992**, *93*, 75. (c) Itoh, N.; Phillips, S. E. V.; Yadav, K. D. S.; Knowles, P. F. *J. Biol. Chem.* **1994**, 238, 794.

10.1021/ic700596g CCC: $37.00
Published on Web 06/27/2007

having salicylidene moieties with two bulky substituents led to a temperature-dependent tautomerism between the Ni(II)−phenoxyl radical and Ni(III)−phenolate states with the same $S = 1/2$ spin state.[9] We previously reported the formation of the phenoxyl radical species by one-electron oxidation of the Ni(II), Cu(II), and Zn(II) complexes of tripodal N_3O ligands derived from *N*-functionalized 2-pyridylmethylamine containing a pendent phenolate moiety with bulky substituents.[10,11] The stability of the Ni(II)−and Cu(II)−phenoxyl radicals from the complexes was found to depend on the donor properties of nitrogen atoms.[8]

On the other hand, the coordination chemistry of transition-metal complexes containing catechols and *o*-benzoquinone ligands has been developed with interesting and surprising results.[12,13] Initial interest in these complexes was associated with the redox activity of quinone ligands.[6,12,13] Especially, Co−catecholate systems showed the valence tautomerism between Co(III)−catecholate and Co(II)−semiquinonate,[12] and detailed properties of some Co(III)−phenoxyl radical species have been reported.[14] In principle, oxidation of complexes containing a phenolate or catecholate ligand can undergo a ligand-centered oxidation generating semiquinonate or phenoxyl radical species, which have multiple radical spins.[14] Further novel oxidation properties are expected for Co(III) complexes containing both catecholate and phenolate ligands.

We have now studied the synthesis of (catecholato)-(phenolato)cobalt(III) complexes of a series of N_3O-donor tripodal ligands with bulky substituents on the phenolate moiety (Figure 1), chemical and electrochemical generation of the one-electron oxidized species, and characterization of their electronic structures by absorption, ESR, and resonance Raman spectroscopies.

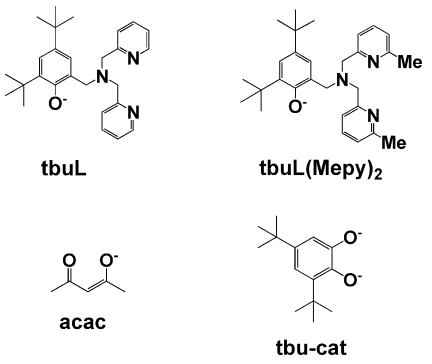

Figure 1. Structures of ligands.

Experimental Section

Materials and Methods. All the chemicals used including 3, 5-di(*tert*-butyl)catechol (H_2tbu-cat) and pentane-2,4-dione (Hacac) ligands (Figure 1) were of the highest grade available and were further purified whenever necessary.[15] Solvents were also purified before use by standard methods.[15] The synthesis of ligands, 2,4-di(*tert*-butyl)-6-{[bis(2-pyridyl)methyl]aminomethyl}phenol (HtbuL), and 2,4-di(*tert*-butyl)-6-{[bis(6-methyl-2-pyridyl)methyl]-aminomethyl}phenolate (HtbuL(Mepy)$_2$) (Figure 1) has been reported previously.[10] Electronic spectra were obtained with a Shimadzu UV-3101PC spectrophotometer. ^{1}H NMR spectra were measured with a JEOL EX-400 spectrometer. Chemical shifts were calibrated relative to tetramethylsilane (TMS) standards. Electrochemical measurements were carried out in a conventional three-electrode cell for samples (1 mM) dissolved in dry CH_3CN containing 0.1 M tetra-*n*-butylammonium perchlorate (TBAP). A glassy-carbon working electrode and a platinum wire as a counter electrode with an Ag/AgCl reference electrode were used in all the experiments. The reversibility of the electrochemical processes was evaluated by standard procedures and referenced against the ferrocene/ferrocenium redox couple. Frozen solution ESR spectra were acquired by a JEOL JES-RE1X X-band spectrometer equipped with a standard low-temperature apparatus. The spectra were recorded by using quartz tubes with a 4-mm inner diameter. Microwave frequency was standardized against a Mn(II) marker. Magnetic susceptibility measurements of Co(II) complexes were performed by Sherwood Scientific MSB-MK1 susceptometer. A diamagnetic correction, estimated from Pascal's constants, was made by subtraction from the experimental susceptibilities to give the molecular paramagnetic susceptibilities. Resonance Raman spectra were obtained on a SpectraPro-300i spectrometer (Acton Research) with a 2400-groove grating, a Beamlok 2060 Kr ion laser (Spectra-Physics), a holographic supernoch filter (Kaiser Optical Systems), and an LN-1100PB CCD detector (Princeton Instruments) cooled with liquid N_2. Spectra were collected on solvated samples in spinning cells (2-cm diameter, 1500 rpm) at −60 °C at an excitation wavelength $\lambda_{ex} = 413.1$ nm (20 mW), 90° scattering geometry, and 5 min data accumulation. Peak frequencies were calibrated relative to toluene standards (accurate to ± 1 cm^{-1}). During each Raman experiment, the UV/vis spectrum was simultaneously collected on a PMA-11 CCD spectrophotometer (Hamamat-

(3) (a) Whittaker, M. M.; Whittaker, J. W.; Milburn, H.; Quick, A. *J. Biol. Chem.* **1990**, *265*, 9610. (b) McGlashen, M. L.; Eads, D. D.; Spiro, T. G.; Whittaker, J. W. *J. Phys Chem.* **1995**, *99*, 4918. (c) Baron, A. J.; Stevens, C.; Wilmot, C.; Seneviratne, K. D.; Blakeley, V.; Dooley, D. M.; Phillips, S. E. V.; Knowles, P. F.; McPherson, M. J. *J. Biol. Chem.* **1994**, *269*, 25095. (d) Knowles, P. F.; Brown, R. D., III; Koenig, S. H.; Wang, S.; Scott, R. A.; McGuirl, M. A.; Brown, D. E.; Dooley, D. M. *Inorg. Chem.* **1995**, *34*, 3895. (e) Reynolds, M. P.; Baron, A. J.; Wilmot, C. M.; Vinecombe, E.; Steven, C.; Phillips, S. E. V.; Knowles, P. F.; MacPerson, M. J. *J. Biol. Inorg. Chem.* **1997**, *2*, 327.
(4) Stubbe, J.; van der Donk, W. A. *Chem. Rev.* **1998**, *98*, 705.
(5) Chaudhuri, P.; Wieghardt, K. *Prog. Inorg. Chem.* **2001**, *50*, 151−216.
(6) (a) Chaudhuri, P.; Verani, C. N.; Bill, E.; Bothe, E.; Weyhermüller, T.; Wieghardt, K. *J. Am. Chem. Soc.* **2001**, *123*, 2213. (b) Herebian, D.; Bothe, E.; Bill, E.; Weyhermüller, T.; Wieghardt, K. *J. Am. Chem. Soc.* **2001**, *123*, 10012.
(7) Shimazaki, Y.; Huth, S.; Odani, A.; Yamauchi, O. *Angew. Chem., Int. Ed.* **2000**, *39*, 1666.
(8) Shimazaki, Y.; Huth, S.; Hirota, S.; Yamauchi, O. *Inorg. Chim. Acta* **2002**, *331*, 168.
(9) (a) Shimazaki, Y.; Tani, F.; Fukui, K.; Naruta, Y.; Yamauchi, O. *J. Am. Chem. Soc.* **2003**, *125*, 10513. (b) Shimazaki, Y.; Yajima, T.; Tani, F.; Karasawa, S.; Fukui, K.; Naruta, Y.; Yamauchi, O. *J. Am. Chem. Soc.* **2007**, *129*, 2559.
(10) Shimazaki, Y.; Huth, S.; Hirota, S.; Yamauchi, O. *Bull. Chem. Soc. Jpn.* **2000**, *73*, 1187.
(11) Shimazaki, Y.; Huth, S.; Karasawa, S.; Hirota, S.; Naruta, Y.; Yamauchi, O. *Inorg. Chem.* **2004**, *43*, 7816−7822.
(12) Pierpont, C. G. *Coord. Chem. Rev.* **2001**, *216-217*, 99.
(13) Evangelio, E.; Ruiz-Molina, D. *Eur. J. Inorg. Chem.* **2005**, 2957.
(14) (a) Sokolowski, A.; Adam, B.; Weyhermüller, T.; Kikuchi, A.; Hildebrandt, K.; Schnepf, R.; Hildebrandt, P.; Bill, E.; Wieghardt, K. *Inorg. Chem.* **1997**, *36*, 3702. (b) Benisvy, L.; Bill, E.; Blake, A. J.; Collison, D.; Davies, E. S.; Garner, C. D.; Guindy, C. I.; McInnes, E. J. L.; McArdle, G.; McMaster, J.; Wilson, C.; Wolowska, J. *Dalton Trans.* **2004**, 3647. (c) Bill, E.; Bothe, E.; Chaudhuri, P.; Chlopek, K.; Herebian, D.; Kokatam, S.; Ray, K.; Weyhermüller, T.; Neese, F.; Wieghardt, K. *Chem. Eur. J.* **2005**, *11*, 204.
(15) Perrin, D. D.; Armarego, W. L. F.; Perrin, D. R. *Purification of Laboratory Chemicals*; Pergamon Press: Elmsford, 1966.

Table 1. Crystal Data for Co(III) Complexes

	3	**4**	**5**
formula	$C_{32}H_{41}N_3O_7CoCl$	$C_{43}H_{57}N_4O_3Co$	$C_{44}H_{60}N_3O_7CoCl_3$
formula weight	674.08	736.88	920.28
color	brown	brown	purple
crystal size/mm	0.11 × 0.04 × 0.02	0.13 × 0.15 × 0.03	0.11 × 0.17 × 0.21
crystal system	monoclinic	orthorhombic	triclinic
space group	$P2_1/a$	*Pccn*	$P\bar{1}$
a (Å)	17.443(3)	32.425(3)	9.248(3)
b (Å)	10.229(2)	25.599(3)	12.351(4)
c (Å)	19.207(4)	10.507(1)	19.719(6)
α/deg			95.78(3)
β/deg	110.090(8)		90.25(2)
γ/deg			95.51(3)
V (Å^3)	3218(3)	8720(3)	2230(3)
Z	4	8	2
μ (Mo Kα) (cm^{-1})	6.67	4.33	6.17
F(000)	1416.00	3152.00	970.00
$2\theta_{max}$ (°)	55.0	54.9	55.0
no. reflections obsd	52958	139152	21452
no. reflections used	7329	9958	9919
no. variables	397	460	523
R {$I = 2\sigma(I)$}	0.065	0.072	0.066
R_w	0.175	0.213	0.227

su Photonics Co.) with a Photal MC-2530 (D_2/W_2) light source (Otsuka Electronic Co.).

Synthesis of Complexes. [Co(tbuL)Cl]•CH$_3$CN (1). To a solution of HtbuL (0.417 g, 1.0 mmol) in CH_3CN (10 mL) was added $CoCl_2$ (0.365 g, 1.0 mmol), and the resulting solution was mixed with a few drops of triethylamine and left to stand for a few days at room temperature under N_2. The dark green microcrystals obtained were recrystallized from CH_3CN. Anal. Found: C, 63.16; H, 6.76; N, 10.14. Calcd for $C_{29}H_{37}N_4OClCo$: C, 63.10; H, 6.76; N, 10.15.

[Co(tbuL(mepy)$_2$)Cl] (2). This complex was prepared in a manner similar to that described for complex **1** using HtbuL(Mepy)$_2$ ligand. Anal. Found: C, 64.61; H, 7.12; N, 7.82. Calcd for $C_{29}H_{38}N_3OClCo$: C, 64.62; H, 7.11; N, 7.80.

[Co(tbuL)(acac)]ClO$_4$ (3). To a solution of **1** (0.055 g, 0.1 mmol) in CH_3CN (10 mL) was added Hacac (0.010 g, 0.1 mmol) and $NaClO_4$ (0.147 g, 0.12 mmol), and the resulting solution was mixed with a few drops of triethylamine, filtered, and left to stand for a few days at room temperature under aerobic conditions. The dark brown microcrystals were recrystallized from CH_3CN. Anal. Found: C, 57.06; H, 6.12; N, 6.24. Calcd for $C_{32}H_{41}N_3O_7ClCo$: C, 57.02; H, 6.13; N, 6.23. ^{1}H-NMR (CD_2Cl_2, 400 MHz, 20 °C): δ = 8.96 (d, 1H), 8.29 (d, 1H), 7.97 (t, 1H), 7.79 (d, 1H), 7.56 (t, 1H), 7.44 (t, 1H), 7.31 (t, 1H), 6.68 (s, 1H), 6.89 (s, 1H), 6.87(d, 1H), 5.70 (s, 1H), 5.26(d, 1H), 4.62 (d, 1H), 4.58 (d, 1H) 4.52 (d, 2H), 4.34 (d, 1H), 2.51 (s, 3H), 2.04 (s, 3H), 1.19 (s, 9H), 1.12 (s, 9H) ppm.

[Co(tbuL)(tbu-cat)]•CH$_3$CN (4). This complex was prepared in a manner similar to that for **3** using a ligand H_2tbu-cat. Anal. Found: C, 70.06; H, 7.82; N, 7.59. Calcd for $C_{43}H_{57}N_4O_3Co$: C, 70.09; H, 7.80; N, 7.60. ^{1}H-NMR (CD_2Cl_2, 400 MHz, 20 °C): δ = 8.71 (d, 2H), 7.59 (t, 2H), 7.20 (t, 2H), 7.13 (m, 4H), 6.71 (s, 1H), 6.69 (d, 1H), 4.31 (d, 2H), 3.43 (m, 4H), 1.43 (s, 9H), 1.22 (s, 9H), 1.19 (s, 9H), 1.12 (s, 9H), 1.05 (s, 9H) ppm.

[Co(tbuL(Mepy)$_2$)(tbu-SQ)]ClO$_4$ (5). This complex was prepared in a manner similar to that for **4** using **2** in methanol. Anal. Found: C, 62.69; H, 7.10; N, 5.12. Calcd for $C_{43}H_{58}N_3O_7ClCo$: C, 62.73; H, 7.10; N, 5.10.

X-ray Structure Determination. The X-ray experiments were carried out for the well-shaped single crystals of all the complexes on a Rigaku RAXIS imaging plate area detector with graphite monochromated Mo Kα radiation (λ = 0.71073 Å). The crystals were mounted on a glass fiber. In order to determine the cell constants and orientation matrix, three oscillation photographs were taken for each frame with the oscillation angle of 3° and the exposure time of 3 min. Reflection data were corrected for both Lorentz and polarization effects. The structures were solved by the heavy-atom method and refined anisotropically for non-hydrogen atoms by full-matrix least-squares calculations. Each refinement was continued until all shifts were smaller than one-third of the standard deviations of the parameters involved. Atomic scattering factors and anomalous dispersion terms were taken from the literature.[16] Hydrogen atoms except for the water were located at the calculated positions and were assigned a fixed displacement and constrained to ideal geometry with C−H = 0.95 Å. The thermal parameters of calculated hydrogen atoms were related to those of their parent atoms by $U(H) = 1.2U_{eq}(C)$. All the calculations were performed by using the TEXSAN program package.[17] Summaries of the fundamental crystal data and experimental parameters for structure determination are given in Table 1.

Results and Discussion

Preparation and Characterization of Mononuclear Cobalt(II) Complexes. The ligand, HtbuL, where H denotes a dissociable proton, reacted with $CoCl_2$ and triethylamine in CH_3CN at room temperature under N_2 to give [Co(tbuL)-Cl]•CH$_3$CN (**1**) as purple crystals. [Co(tbuL(mepy)$_2$)Cl] (**2**) was obtained from a similar reaction of **1** as brown crystals. The ORTEP views of complexes **1** and **2** are shown in Figure S1, and the selected bond lengths and angles are listed in Table S2 in the Supporting Information. The structure of **1** has a trigonal bipyramidal geometry formed by a phenolato oxygen, two pyridine nitrogens, a tertiary nitrogen, and a chloride ion with the distances, Co−O(1) = 1.914(1), Co−N(1) = 2.090(2), Co−N(2) = 2.201(2), and Co−N(3) = 2.090(2) Å, respectively. The trigonal plane was composed

(16) *International Tables for X-ray Crystallography*; Ibers, J. A., Hamilton, W. C., Eds.; Kynoch: Birmingham, 1974; Vol. IV.
(17) *Crystal Structure Analysis Package*; Molecular Structure Corporation: 1985 and 1999.

of two pyridine nitrogens, N(1) and N(3), and a phenolate oxygen, the Co−N(1) and Co−N(3) distances being shorter than the axial Co−N(2) distance. The geometry of complex **2** was also found to be trigonal bipyramidal, whose trigonal plane was different from that of **1** and composed of a phenolate oxygen, a tertiary amine nitrogen, and a chloride ion with the distances Co−O(1) = 1.923(1), Co−N(2) = 2.114(2), and Co−Cl = 2.301(1) Å, respectively. The two 2-methylpyridine nitrogens are bound at axial positions, since the donor ability of 2-methylpyridine moiety is lower than that of unsubstituted pyridine donor.[10,11,18] This tendency was observed in the Ni(II) complex of the same ligand.[11]

Complexes **1** and **2** were determined to be paramagnetic d^7 high-spin, $S = 3/2$ Co(II) species from their effective magnetic moments (μ_{eff}) of the monomeric complexes 3.70 and 3.92 μ_B at 298 K, respectively, which were in good agreement with the theoretical value based on $S = 3/2$ state ($\mu_{eff} = 3.87\ \mu_B$) from the spin-only equation. No sharp ^{1}H-NMR spectra were observed in the diamagnetic region. However, the absorption spectra of **1** and **2** were different from each other, indicating the difference in the coordination geometry. Complex **1** showed absorption bands at λ (ϵ M^{-1}•cm^{-1}) = 812 (30), 604 (290), 552 (210), 495 (150), and 386 (sh, 1260) nm in CH_3CN. The 604-, 552-, and 495-bands are considered as the d−d transition bands, and the 386-nm band is assigned to the phenolate to Co(II) charge transfer.[19,20] In contrast to this, **2** showed absorption bands centered at 565 (br, 100) and 415 (900) nm, which are different from those of **1**, indicating that the structural difference between **1** and **2** was maintained in solution. The structural difference in solution was also reflected on their redox properties. Complexes **1** and **2** exhibited two pseudoreversible redox waves at $E_{1/2} = 0.34$ and 1.09 V and 0.62 and 1.08 V vs Ag/AgCl, respectively. Though the second waves of **1** and **2** showed similar $E_{1/2}$ values, the first potential of **2** was much higher than that of **1**. While the coordination structure affects the ligand-centered oxidation process only weakly, it strongly influences the oxidation potential of the metal ion. Therefore, the first potential is assigned to the Co(II)/Co(III) redox process and the second one to the phenolate/phenoxyl radical redox process, reflecting the difference in the structures in solution. The redox potential difference between **1** and **2** may be partly due to the difficulty in contraction in **2** for steric reasons arising from the presence of the methyl group in the pyridine 6 position.[18]

Preparation and Crystal Structures of Mononuclear Cobalt(III) Complexes. Though Co(II) complexes **1** and **2** were stable in solution under aerobic conditions, these were easily oxidized under aerobic conditions in the presence of a 2O-bidentate ligand, such as Hacac and H_2tbu-cat, and triethylamine. Complex **1** reacted with Hacac, $NaClO_4$, and triethylamine in CH_3CN at room temperature under aerobic conditions to give [Co(tbuL)(acac)]ClO_4 (**3**) as dark brown crystals. A neutral catecholate complex [Co(tbuL)(tbu-cat)]•CH_3CN (**4**) was obtained by a similar reaction of **1** with H_2tbu-cat as brown crystals. Complex **2** reacted with H_2tbu-cat and triethylamine in CH_3OH at room temperature to give [Co(tbuL(mepy)$_2$)(tbu-SQ)]ClO_4 (**5**) as dark purple crystals. The ORTEP view of **3** is shown in Figure 2 and those of **4** and **5** are in Figure 3, and the selected bond lengths and angles are listed in Table 2. The structure of **3** has an octahedral geometry formed by one phenolate oxygen, two

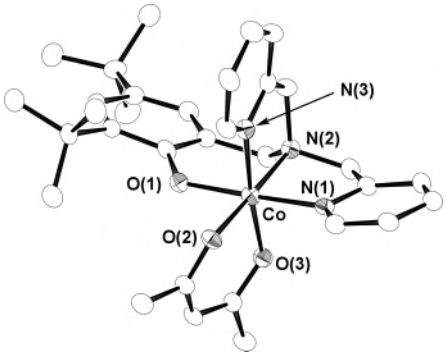

Figure 2. ORTEP view of [Co(tbuL)(acac)]$^+$ ion in complex **3** drawn with the thermal ellipsoids at the 50% probability level and atomic labeling scheme.

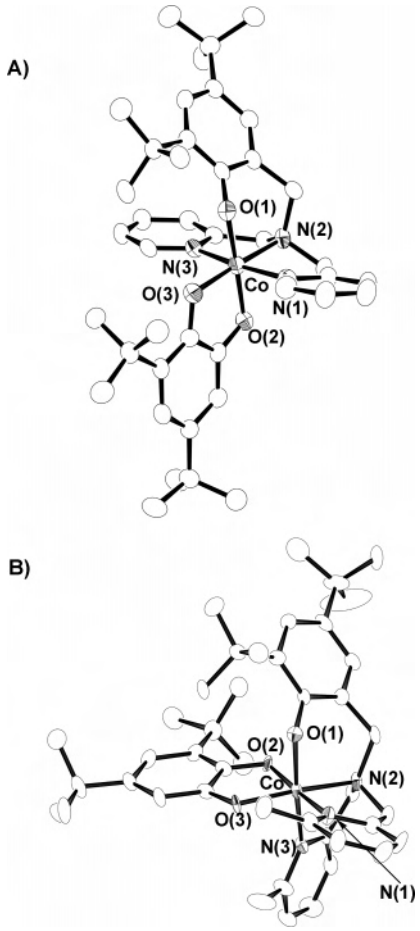

Figure 3. ORTEP views of [Co(tbuL)(tbu-cat)] (**4**) and [Co(tbuL(mepy)$_2$)(tbu-SQ)]$^+$ ion in complex **5** drawn with the thermal ellipsoids at the 50% probability level and atomic labeling scheme: (A) [Co(tbuL)(tbu-cat)] (**4**), and (B) [Co(tbuL(mepy)$_2$)(tbu-SQ)]$^+$ ion in complex **5**.

(18) Nagao, H.; Komeda, N.; Mukaida, M.; Suzuki, M.; Tanaka, K. *Inorg. Chem.* **1996**, *35*, 6809.
(19) Hitchman, M. A. *Inorg. Chem.* **1977**, *16*, 1985.
(20) Kasumov, V. T.; Özdemir, M.; Tas, E.; Sahin, Ö. *Trans. Met. Chem.* **2005**, *30*, 191.

Table 2. Selected Bond Distances (Å) and Angles (deg) of Co(III) Complexes **3**−**5**

	3	4	5
		Distances	
Co(1)−O(1)	1.873(3)	1.920(3)	1.912(2)
Co(1)−O(2)	1.903(3)	1.875(3)	1.918(2)
Co(1)−O(3)	1.889(3)	1.886(3)	1.916(2)
Co(1)−N(1)	1.944(4)	1.928(4)	2.009(3)
Co(1)−N(2)	1.963(4)	1.957(4)	1.942(2)
Co(1)−N(3)	1.918(4)	1.924(4)	1.965(2)
		Angles	
O(1)−Co(1)−O(2)	85.3(1)	87.7(1)	90.13(9)
O(1)−Co(1)−O(3)	91.3(1)	175.6(1)	91.79(9)
O(1)−Co(1)−N(1)	177.4(1)	94.4(1)	172.40(9)
O(1)−Co(1)−N(2)	94.5(1)	94.7(1)	94.3(1)
O(1)−Co(1)−N(3)	91.4(1)	88.8(1)	88.32(9)
O(2)−Co(1)−O(3)	93.7(1)	88.3(1)	83.94(8)
O(2)−Co(1)−N(1)	94.5(1)	95.3(1)	85.47(9)
O(2)−Co(1)−N(2)	178.7(1)	177.3(1)	93.41(9)
O(2)−Co(1)−N(3)	91.6(1)	95.3(1)	177.66(9)
O(3)−Co(1)−N(1)	90.8(1)	88.0(1)	93.9(1)
O(3)−Co(1)−N(2)	87.6(1)	89.2(1)	173.39(9)
O(3)−Co(1)−N(3)	174.0(1)	89.5(1)	97.85(9)
N(1)−Co(1)−N(2)	85.6(2)	85.6(1)	79.8(1)
N(1)−Co(1)−N(3)	86.0(2)	169.0(2)	95.9(1)
N(2)−Co(1)−N(3)	87.0(2)	83.7(2)	85.0(1)

pyridine nitrogens, a tertiary nitrogen, and two acac oxygen atoms (Figure 2). Three nitrogen atoms of **3** give a *fac*-configuration with the Co−O and Co−N bond distances, Co−O(1) = 1.873(3), Co−O(2) = 1.903(3), Co−O(3) = 1.889(3), Co−N(1) = 1.944(4), Co−N(2) = 1.963(4), and Co−N(3) = 1.918(4) Å, respectively, the Co−N(2)(tertiary nitrogen) bond distance being slightly longer than the Co−pyridine nitrogen distances (Table 2). The Co−O(phenolate) bond (1.873(3) Å) is very short in comparison with the values for the known phenolate cobalt(III) complexes.[21] Complex **4** has an octahedral geometry formed by a phenolate oxygen, two pyridine nitrogens, a tertiary nitrogen, and two catecholate oxygen atoms (Figure 3A). Three nitrogen atoms of **4** show a *mer*-configuration with the Co−O and Co−N bond distances, Co−O(1) = 1.920(3), Co−O(2) = 1.875(3), Co−O(3) = 1.886(3), Co−N(1) = 1.928(4), Co−N(2) = 1.957-(4), and Co−N(3) = 1.924(4) Å, respectively. The Co−O(phenolate) bond length in **4** (1.920(3) Å) is longer than that of **3** (1.873(3) Å), but the Co−N(1) distance (1.928(4) Å) is slightly shorter than that of **3** (1.944(4) Å), probably due to the trans effect in **4**. The structure of **5** (Figure 3B) is similar to that of **3** as it has an octahedral geometry formed by one phenolate oxygen, two pyridine nitrogens, one tertiary nitrogen, and two catecholate oxygen atoms. Three nitrogen atoms of **5** give a *fac*-configuration with the Co−O and Co−N bond distances, Co−O(1) = 1.912(2), Co−O(2) = 1.918(2), Co−O(3) = 1.916(2), Co−N(1) = 2.009(3), Co−N(2) = 1.942(2), and Co−N(3) = 1.965(2) Å, respectively. The Co−N(pyridine) bonds of **5** are longer than those of **3** and **4** and the Co−N(amine) bond of **5**, because of the steric reason of the methyl group in 2-methylpyridine.[10,11,18] This tendency has been observed for Co(II) complexes **1** and **2** and other metal complexes of the same ligand series.[10,11]

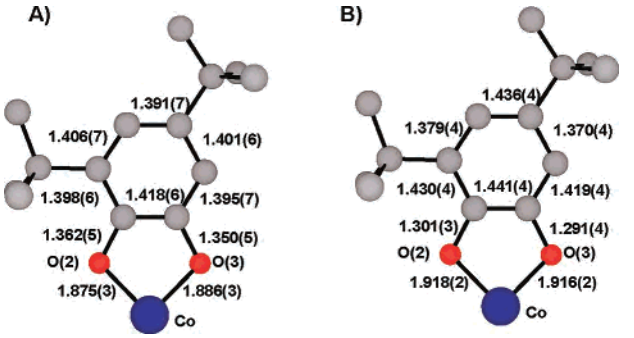

Figure 4. Dioxolene ligand bond lengths of **4** and **5**: (A) complex **4** and (B) complex **5**.

The C−O bond distances of the bidentate oxygen ligand moiety in **5** are significantly shorter than those in **4** (Figure 4), and also, the three C−C bonds adjacent to the C−O bonds of the oxygen ligand in **5** are significantly longer than the corresponding bonds in **4**. These structural features revealed that **4** contains a catecholate ligand, whereas **5** has a semiquinonate ligand.[22] A shortening of the C−O and the lengthening of the three adjacent C−C bonds in **5** are in accord with the description of the two resonance forms of the electronic structure of the semiquinonate ligand, whose unpaired electron is delocalized over the *ortho* oxygens. The structural characteristics of **5** were similar to those of other reported semiquinonato−metal complexes.[12,13,22]

Characterization of Co(III)−Phenolate Complexes. Complexes **3** and **4** are diamagnetic, whereas complex **5** is paramagnetic due to the semiquinonate ligand. The ^{1}H NMR spectrum of **3** in CH_3CN showed 8 different pyridine proton signals, indicating that the two pyridine moieties are distinguishable; that is, the *fac*-N_3O_3 configuration is maintained in solution. On the other hand, the ^{1}H NMR of **4** exhibited from pyridine proton signals, which suggests that the two pyridine moieties are equivalent in solution. Complex **4** is thus inferred to have the *mer*−N_3O_3 configuration in solution as in the solid state (Figure S2 in the Supporting Information). Complex **3** exhibited two absorption peaks in the range 300−1100 nm (λ_{max} (ϵ/M^{-1} cm^{-1}): 455 (2400), 636 (1300) nm) in CH_3CN. The band at 636-nm band is assigned to the d−d band of *fac*-N_3O_3 configuration.[23] Complex **4** having the coordinated phenolate and catecholate oxygens showed some broad shoulder bands at 410 (sh, 3000), 550 (sh, 500), and 700 (sh, 300) nm. It did not show the clear d−d band in the absorption spectrum, indicating that it maintained a *mer*-configuration in solution, and the results agreed well with the result of the NMR study.[23,24] On the other hand, complex **5** was found to be paramagnetic $S = 1/2$ species with the effective magnetic moment of $\mu_{eff} = 1.70$ μ_{BM}. The ESR spectrum of **5** in CH_2Cl_2 showed an isotropic signal at $g = 2.00$ with the hyperfine structure due to interaction of the semiquinonate with ^{59}Co ($I = 7/2$), whose A value was determined to be 1.1 mT (Figure S3 in the Supporting

(21) Riley, P. E.; Pecoraro, V. L.; Carrano, C. J.; Raymond, K. N. *Inorg. Chem.* **1983**, *22*, 3096.
(22) Adams, D. M.; Dei, A.; Rheingold, A. L.; Hendrickson, D. N. *J. Am. Chem. Soc.* **1993**, *115*, 8221.
(23) Shakya, R.; Imbert, C.; Hratchian, H. P.; Lanznaster, M.; Heeg, M. J.; McGarvery, B. R.; Allard, M.; Schlegel, H. B.; Verani, C. N. *Dalton Trans.* **2006**, 2517.
(24) Chakravorty, A.; Behera, B. *Inorg. Chem.* **1967**, *6*, 1812.

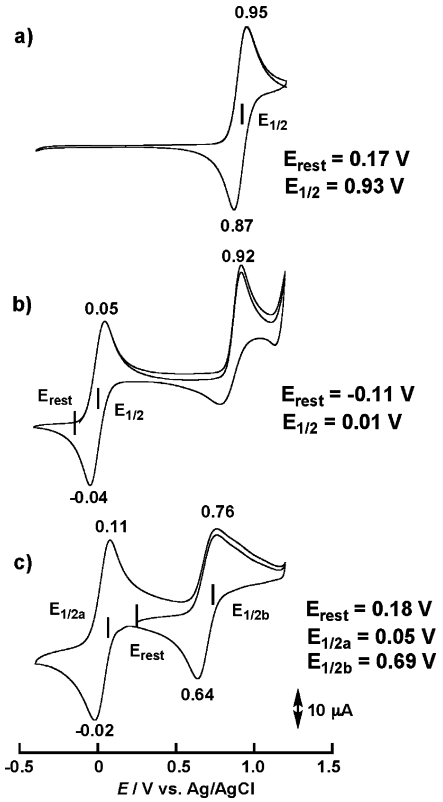

Figure 5. Cyclic voltammograms of **3**−**5** in CH_3CN (1.0 mM) containing 0.1 M *n*-Bu_4NClO_4: (a) **3**, (b) **4**, and (c) **5**. Working electrode, glassy carbon; counter electrode, Pt wire; reference electrode, Ag/AgCl; scan rate 50 mV s^{-1}.

Infomation). These results indicate that the catecholate ligand was oxidized to semiquinonate.[25,26] The absorption spectrum of **5** in CH_2Cl_2 showed strong bands centered at 385 (3800), 518 (3000), and 700 (2100) nm. This spectral feature, especially the intense 385-nm band, is different from the bands of **3** and **4** and is assigned to a semiquinonate $\pi-\pi^*$ transition band.

The cyclic voltammograms of **3**−**5** were recorded in CH_3CN under anaerobic conditions at a scan rate of 50 mV s^{-1} in the range −0.5−1.2 V (Figure 5). For complex **3**, one reversible redox wave corresponding to the transfer of one electron was observed at 0.93 V vs Ag/AgCl (ΔE = 0.08 V). On the other hand, complexes **4** and **5** showed two oxidation peaks; one reversible redox wave at 0.11 V and one irreversible oxidation peak at 0.92 V were observed for **4**, while two quasi-reversible redox waves were observed for **5** at 0.05 and 0.69 V. The rest potential, which corresponds to the potential of **4** itself (E_{rest} = 0.11 V), is lower than the first reversible redox wave, whereas that of **5** (E_{rest} = 0.18 V) was higher than the first redox process. Since the redox wave around 0 V was not observed for **3**, the lower redox waves of **4** and **5** around 0 V are inferred to be due to the catechol/semiquinonate redox process.

One-Electron Oxidation of Complex 3. Electrolysis at 1.2 V of a solution of **3** in CH_3CN or CH_2Cl_2 (0.1 M TBAP) at −20 °C caused a transfer of 0.9 electron per molecule and a color change to dark blue. The properties of oxidized **3** were the same irrespective of the methods of oxidation, electrochemical oxidation or chemical oxidation by addition of 1 equiv of Ce(IV) ion. As a result of the oxidation, the phenolate to Co(III) charge-transfer band in the absorption spectrum disappeared, and a new strong band appeared at 412 nm (Figure 6). The oxidation yielded an ESR active species with an isotropic signal at g = 2.00 without hyperfine coupling of Co ion (Figure S3 in the Supporting Information). The resonance Raman spectrum of oxidized **3** exhibited bands at 1476, 1488, and 1597 cm^{-1} (Figure 7). For metal-coordinated phenoxyl radicals, the frequency difference, $\nu_{8a} - \nu_{7a}$, and the Raman intensity ratio, $I(\nu_{8a})/I(\nu_{7a})$, have been reported to be >90 cm^{-1} and >1, respectively,[27] while the uncoordinated radical exhibits the frequency difference of <90 cm^{-1} and the intensity ratio of <0.1.[27,28] The band at

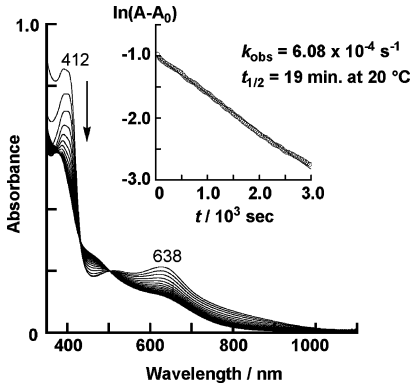

Figure 6. Absorption spectral change of **3** after one-electron oxidation by 1 equiv of Ce(IV) at 20 °C in CH_3CN (5.0×10^{-4} M). Inset: plot of $\ln[A-A_0]$ at 412 nm vs time.

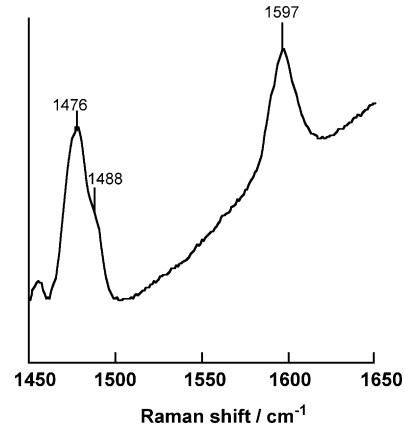

Figure 7. Resonance Raman spectrum of one-electron oxidized **3** (2.0 mM in CH_2Cl_2) with 413.1-nm excitation using an Ar^+ laser (power: 20 mW at the sample point).

(25) (a) Buchanan, R. M.; Pierpont, C. G. *J. Am. Chem. Soc.* **1980**, *102*, 4951. (b) Wicklund, P. A.; Beckmann, L. S.; Brown, D. G. *Inorg. Chem.* **1976**, *15*, 1996. (c) Lange, C. W.; Conklin, B. J.; Pierpont, C. G. *Inorg. Chem.* **1994**, *33*, 1276.

(26) Kessel, S. L.; Emberson, R. M.; Debhrunner, P.; Hendrickson, D. N. *Inorg. Chem.* **1980**, *19*, 1170.

(27) (a) Sokolowski, A.; Leutbecher, H.; Weyhermüller, T.; Schnepf, R.; Bothe, E.; Bill, E.; Hildebrandt, P.; Wieghardt, K. *J. Biol. Inorg. Chem.* **1997**, *2*, 444. (b) Sokolowski, A.; Müller, J.; Weyhermüller, T.; Schnepf, R.; Bill, E.; Hildebrandt, P.; Hildenbrand, K.; Bothe, E.; Wieghardt, K. *J. Am. Chem. Soc.* **1997**, *119*, 8889.

(28) (a) McGlashen, M. L.; Eads, D. D.; Spiro, T. G.; Whittaker, J. W. *J. Phys. Chem.* **1995**, *99*, 4918. (b) Babcock, G. T.; El-Deeb, M. K.; Sandusky, P. O.; Whittaker, M. M.; Whittaker, J. W. *J. Am. Chem. Soc.* **1992**, *114*, 3727.

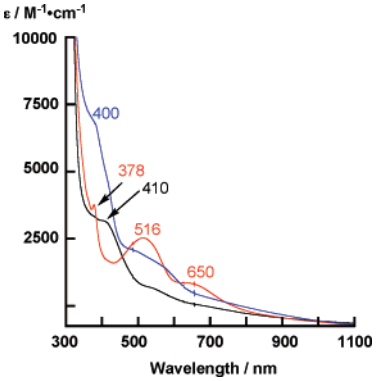

Figure 8. Absorption spectral change of **4** after one-electron oxidation by 1 and 2 equiv of Ce(IV) at −60 °C in CH_2Cl_2 (5.0×10^{-4} M): black line, **4**; red line, one-electron oxidized **4**; blue line, two-electron oxidized **4**.

1597 cm^{-1} is readily assigned to the ν_{8a} stretching mode of the metal coordinated phenoxyl radical, and the weak shoulder at 1488 cm^{-1} near the 1476-cm^{-1} peak is attributable to the ν_{7a} mode. On the basis of these results, we assign the above oxidation step at 0.93 V to the coordinated phenolate/phenoxyl radical couple.

When the blue solutions of oxidized **3** in CH_2Cl_2 were left to stand at room temperature under anaerobic conditions, they rapidly turned brown, and accordingly the phenoxyl radical $\pi-\pi^*$ transition band at 412 nm disappeared (Figure 6). Plot of the absorbance at the $\pi-\pi^*$ band vs time at 20 °C indicated that the intensity decrease was in first-order as illustrated for **3** (Figure 6, inset). The half-life of oxidized **3** was 19.0 min ($k_{obs} = 6.08 \times 10^{-4}$ s^{-1}) at 20 °C, indicating that the stability of phenoxyl radical is comparable with those for the Ni(II) complex with the same N_3O chelating ligand.[11] The final decay products of oxidized **3** were mainly 3,5-di(*tert*-butyl)salicylaldehyde (more than 5% as isolated) together with some other unidentified compounds. Detection of 3,5-di(*tert*-butyl)salicylaldehyde as a final product suggests the formation of the phenoxyl radical species in the course of the decay.

Characterization of Oxidized 4 and 5. Addition of 1 equiv of $(NH_4)_2Ce(NO_3)_6$, one electron oxidant, to **4** in CH_3CN at room temperature caused a color change from brown to purple. The color change was also observed on the electrochemical oxidation at 0.4 V. One-electron oxidized **4** exhibited new intense absorption bands at 378 (3800), 516 (2500), and 650 (900) nm (Figure 8). The spectrum was very similar to that of **5**. The intense transition band at 378 nm may be partly assigned to a $\pi-\pi^*$ transition of the semiquinonate radical, and the spectral features are in good agreement with those of the Co(III)−semiquinonate complexes reported.[25,26] The ESR spectra of the one-electron oxidized species at 77 K exhibited an isotropic signal at $g = 2.00$ with hyperfine structure due to the ^{59}Co ion $A = 1.1$ mT (Figure S3 in the Supporting Information). The oxidation level of **4** is the same as that of **5**. Two-electron oxidized **4** was not so stable in CH_2Cl_2 at −60 °C. Its decay constant was estimated to be $k_{obs} = 1.13 \times 10^{-3}$ s^{-1} ($t_{1/2} = 613$ s), which indicates that it is of lower stability than the phenoxyl radical nickel(II) and copper(II) complexes with

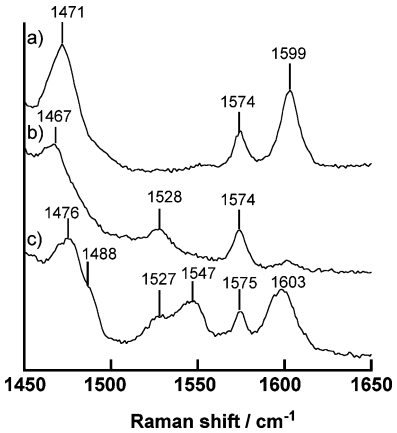

Figure 9. Resonance Raman spectra of (a) **4**, (b) one-electron oxidized **4**, and (c) two-electron oxidized **4** obtained for 2 mM solutions in CH_3CN: 413.1-nm excitation using an Ar^+ laser (power: 20 mW at the sample point).

similar N_3O tripodal ligands.[10,11] The ESR spectrum of two-electron oxidized **4** was silent at 5 K. This ESR feature is different from that of the reported Co(III) complex with weak ferromagnetic coupling between the phenoxyl radical and semiquinonate unpaired electrons showing the anisotropic signals at $g = 4$ and 2 at low temperature.[14] The present result may indicate that the two-electron oxidized species has an $S = 0$ ground state. The resonance Raman spectra of **4** before and after oxidation (Figure 9) indicate that one-electron oxidized **4** exhibits a new Raman band at 1528 cm^{-1}, which is also observed for **5**. In the cases of the other reported Co(III) semiquinonate complexes, this band has been assigned to the ν_{8a} vibration of the semiquinonate.[14,26,29] The Raman spectrum of two-electron oxidized **4** showed the ν_{8a} band of the semiquinonate at 1528 cm^{-1} and new bands at 1488, 1547, and 1603 cm^{-1}. The 1488- and 1603-cm^{-1} bands correspond well with the 1488- and 1597-cm^{-1} bands of one-electron oxidized **3** as ν_{7a} and ν_{8a} bands of Co(III) coordinated phenoxyl radical, respectively. Therefore, two-electron oxidized **4** is assigned to a Co(III)-semiquinonate phenoxyl radical complex with strong antiferromagnetic coupling between the semiquinonate and phenoxyl radical unpaired electrons. One of the reasons of the antiferromagnetic interaction may be that the phenoxyl radical oxygen is situated in the *trans*-position of the semiquinonate oxygen. Since Co(III) complexes are generally inert toward the ligand exchange, the two-electron oxidized form of **4** is considered to have a geometry similar to that of unoxidized **4** revealed by X-ray analysis. The two unpaired electrons may be exchangeable through the same orbital of the Co(III) ion. On the other hand, each unpaired spin could be in an orthogonal arrangement, since a ferromagnetically coupled Co(III)−semiquinonate phenoxyl radical complex has been reported to have the *mer*-N_3O_3 geometry.[14]

One-electron oxidized semiquinonate complex **5** exhibited a new intense absorption band at 408 (3800) nm with the intensity decrease of the peaks at 519 (2000) and 703 (1000) nm (Figure 10) and was ESR inactive at 5 K. In the resonance Raman spectrum of one-electron oxidized **5**

(29) Matsunaga, Y. *J. Chem. Phys.* **1964**, *41*, 1609.

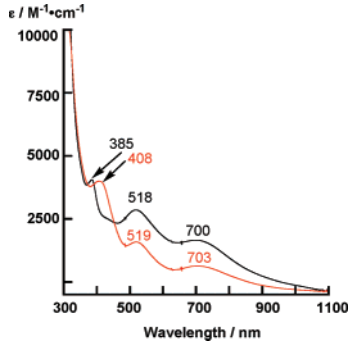

Figure 10. Absorption spectral change of **5** after one-electron oxidation by 1 equiv of Ce(IV) at −60 °C in CH_2Cl_2 (5.0×10^{-4} M): black line, complex **5**; red line, one-electron oxidized **5**.

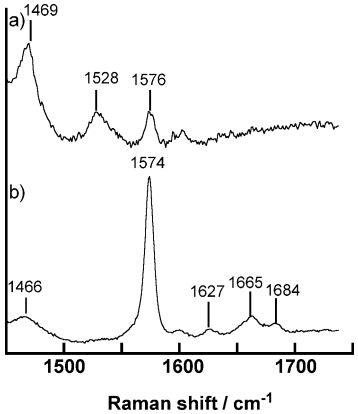

Figure 11. Resonance Raman spectra of (a) **5** and (b) one-electron oxidized **5** obtained for 2.0 mM solutions in CH_3CN: 413.1-nm excitation using an Ar^+ laser (power: 20 mW at the sample point).

(Figure 11), the semiquinonate ν_{8a} vibration at 1528 cm^{-1} disappeared, and two new bands appeared at 1665 and 1684 cm^{-1}. An additional intense band was also observed at 1574 cm^{-1}. The *o*-quinones are normally characterized by the C═O stretching frequencies ranging from 1660 to 1700 cm^{-1};[29] for example, 3,5-di(*tert*-butyl)quinone in CCl_4 shows two carbonyl bands at 1670 and 1695 cm^{-1}.[30] The Raman feature suggests that oxidized **5** is a Co(III)-(phenolate)(quinone) complex, which is different from that of two-electron oxidized **4**, a Co(III)(phenoxyl)(semiquinonate) complex. One-electron oxidized **5** was stable at −20 °C but showed a gradual color change to brown at room temperature, the decay constant being estimated to be $k_{obs} = 1.70 \times 10^{-6}$ s^{-1} ($t_{1/2} = 11.3$ h) at 20 °C.

The different electronic structures of oxidized Co(III)-(phenoxyl)(semiquinonate) of **4** and **5** indicate that the redox potential of the phenolate moiety is predominantly influenced by the N-donor ability of the ligand stabilizing the Co(III) state, which corresponds with the finding on the Cu(II)− and Ni(II)−phenoxyl radical complexes.[10,11] We reported previously that the phenolate/phenoxyl radical redox potential for the Cu(II) and Ni(II) complexes corresponding to **5** with two *o*-methylpyridine rings was higher than that of the complex with one pyridine and one *o*-methylpyridine.[10,11] This may indicate that the equatorial 2-methylpyridine ring is a weaker donor than the unsubstituted pyridine probably for steric reasons. More electron-deficient complex **5** requires a higher potential for phenoxyl radical formation than that for **4**, and therefore the semiquinonate ligand may be oxidized.

Conclusion

We prepared and characterized a series of Co(II) complexes with N_3O-donor tripodal ligands containing one phenolate moiety with two *tert*-butyl substituents and two pyridine rings with and without a methyl group *ortho* to the nitrogen atom. Co(III)(phenolate), Co(II)(catecholate)(phenolate), and Co(III)(semiquinonate)(phenolate), were synthesized by the reaction of Co(II) complexes **1** and **2** as building blocks with O_2-donor chelating ligands, Hacac and 3,5-di(*tert*-butyl)catechol (thu-cat). At low temperatures, one-electron oxidation of all the Co(III)(acac) complex yielded the corresponding Co(III)−phenoxyl radical species, whose decay constants have been determined. Further, one- or two-electron oxidized Co(III)(catecholate)(phenolate) and one-electron oxidized Co(III)(semiquinonate)(phenolate) were characterized. One- and two-electron oxidations of *fac*-N_3O_3 Co(III)(catecholate)(phenolate) complex showed the stepwise ligand-centered oxidation to give Co(III)(semiquinonate)-(phenolate) and Co(III)(semiquinonate)(phenoxyl) complexes, respectively. On the other hand, one-electron oxidation of the *mer*-N_3O_3 Co(III)(semiquinonate)(phenolate) complex did not give the phenoxyl radical species, but the Co(III)(quinone)(phenolate) complex was formed instead. The relationship between the structures of the complexes and their oxidation behavior indicated that the oxidation center is dependent on the properties of the pyridine nitrogen donors. These results illustrate the control of the oxidation locus that can be reached by modulating the ligand field, as observed in some Ni complexes.[9,31,32] Further studies on the metal−phenoxyl binding are in progress in our laboratory.

Acknowledgment. The present work was supported by Grants-in-Aid for Scientific Research (No. 17750055 to Y.S. and No. 16350036 to O.Y.) from the Ministry of Education, Culture, Sports, Science, and Technology of Japan.

Supporting Information Available: Crystallographic data (excluding structure factors) for complexes **1**−**5** in CIF format, crystal data of Co(II) complexes (Table S1), selected bond distances and angles (Table S2), ORTEP views of Co(II) complexes (Figure S1), ^1H NMR spectra of complexes **3** and **4** in CD_2Cl_2 (Figure S2), and ESR spectra of **5** and one-electron oxidized **3** and **4** in CH_2Cl_2 at 77 K (Figure S3). This material is available free of charge via the Internet at http://pubs.acs.org.

IC700596G

(30) Rieker, A.; Rundel, W.; Kessler, H. Z. *Naturforsch., B: Chem. Sci.* **1969**, *24*, 547.
(31) (a) Ohtsu, H.; Tanaka, K. *Angew. Chem., Int. Ed.* **2004**, *43*, 6301. (b) Ohtsu, H.; Tanaka, K. *Chem. Eur. J.* **2005**, *11*, 3420.
(32) (a) Rotthaus, O.; Jarjayes, O.; Thomas, F.; Philouze, C.; Perez, del Valle, C.; Saint-Aman, E.; Pierre, J.-L. *Chem. Eur. J.* **2006**, *12*, 2293. (b) Rotthaus, O.; Thomas, F.; Jarjayes, O.; Philouze, C.; Saint-Aman, E.; Pierre, J.-L. *Chem. Eur. J.* **2006**, *12*, 6953.